THE JOURNAL OF PHYSICAL CHEMISTRY C

Article

pubs.acs.org/JPCC

Identification of Nonequivalent Framework Oxygen Species in Metal–Organic Frameworks by ^{17}O Solid-State NMR

Peng He,[†] Jun Xu,[†] Victor V. Terskikh,[‡] Andre Sutrisno,[†] Heng-Yong Nie,[§] and Yining Huang*,[†]

[†]Department of Chemistry, The University of Western Ontario, London, Ontario, Canada N6A 5B7

[‡]National Research Council Canada, 100 Sussex Drive, Ottawa, Ontario, Canada K1A 0R6

[§]Surface Science Western, The University of Western Ontario, London, Ontario, Canada N6G 0J3

Supporting Information

ABSTRACT: Metal–organic frameworks (MOFs) are a class of novel nanoporous materials with many potential applications. Structural characterization is important because understanding the relationship between the properties of these industrially relevant materials and their structures allows one to develop new applications and improve current performance. Oxygen is one of the most important elements in many MOFs and exists in various forms. Ideally, ^{17}O solid-state NMR (SSNMR) should be an excellent tool for characterizing various oxygen species. However, the major obstacles that prevent applying ^{17}O SSNMR to MOF characterization are the synthetic effort needed for ^{17}O isotopic enrichment and the associated high cost. In this work, we successfully prepared several prototypical ^{17}O-enriched MOFs, including Zr-UiO-66, MIL-53(Al), CPO-27-Mg (or Mg-MOF-74), and microporous α-$Mg_3(HCOO)_6$. Depending on the target MOF, different isotopic enrichment methods were used to effectively incorporate ^{17}O from ^{17}O-enriched H_2O. Using these ^{17}O-enriched MOFs, we were able to acquire ^{17}O SSNMR spectra at a magnetic field of 21.1 T. They provide distinct spectral signatures of various key oxygen species commonly seen in representative MOFs. We demonstrate that ^{17}O SSNMR can be used to differentiate chemically and, under favorite circumstances, crystallographically nonequivalent oxygens and to follow the phase transitions. The synthetic approaches for preparation of ^{17}O-enriched sample described in this paper are fairly simple and cost-effective.

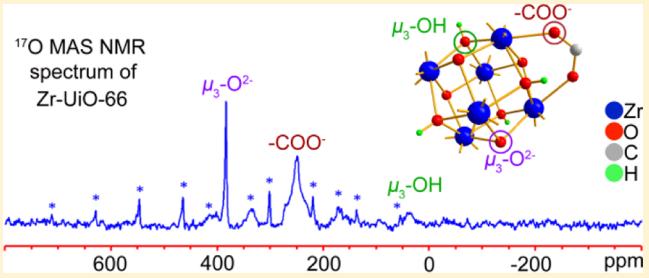

INTRODUCTION

One of the most exciting advances in the field of porous materials in recent years is the emergence of a family of hybrid organic–inorganic solids known as metal–organic frameworks (MOFs).[1] MOFs are prepared via self-assembly of metal cations with organic linkers to form 3D networks with novel topologies. They have high thermal stability, permanent porosity, a flexible framework, and exceptionally high surface areas, leading to many potentially important applications in areas such as ion-exchange, catalysis, molecular recognition, drug delivery, and in particular gas separation and storage. Detailed structural characterization of these industrially relevant materials is important because understanding the relationship between their properties and the structures allows one to develop new applications and improve current performance. Although the structures of many MOFs can be determined by single-crystal X-ray diffraction, a significant number of MOF structures have to be refined from more limited powder XRD data due to the lack of suitable single crystals. Activation/desolvation may reduce the crystallinity. In such cases a reliable structure solution requires additional information from complementary techniques such as solid-state NMR (SSNMR). Indeed, SSNMR has been used extensively for MOF characterization.[2,3] ^{1}H and ^{13}C SSNMR spectroscopy has been routinely used for characterization of organic linkers.[4−8] ^{2}H NMR is employed to examine the flexibility of the framework and the dynamics of the guest species.[9,10] ^{129}Xe NMR has been utilized to study the porosity in the MOF frameworks.[11−13] Very recently, the utility of DNP (dynamic nuclear polarization)-enhanced ^{13}C and ^{15}N SSNMR in MOF characterization has been demonstrated.[14] SSNMR of several metal centers such as ^{27}Al,[7,15,16] ^{45}Sc,[17] ^{71}Ga,[18] ^{25}Mg,[19,20] and ^{67}Zn[21] has been employed to directly characterize the local structures around metal centers.

The oxygen present in various carboxylate ligands is a key constituent of many MOFs. Certain MOFs have framework hydroxyl species[15,22] and water molecules directly bound to the metal center[23] as well as oxygen anions (O^{2-}) associated with the metal clusters.[22] Some organic linkers have phenol groups and the phenol oxygen can bind to a metal ion upon deprotonation.[23] Ideally ^{17}O SSNMR should be utilized for characterization of different oxygen species because ^{17}O exhibits a large chemical shift range and is also sensitive to both the electric field gradient (EFG) and the chemical shielding (CS) tensors.[24−28] However, ^{17}O SSNMR work on MOFs has been

Received: April 9, 2013
Revised: June 17, 2013
Published: June 19, 2013

very rare due to the very low natural abundance (0.037%) of ^{17}O. To the best of our knowledge, there is only one recent report which showed that it is possible to incorporate ^{17}O into specific sites in MOF-5 structures.[29]

In the present work, using several synthetic strategies, we were able to directly synthesize several ^{17}O-enriched MOFs with ^{17}O-enriched water as the ^{17}O source, including MIL-53(Al),[15] Zr-UiO-66,[22] CPO-27-Mg[23] (also known as MOF-74[30−32]), and microporous α-$Mg_3(HCOO)_6$.[33] The reason for choosing these MOFs is that they are among the most important and frequently examined MOF systems with unique structure features. By acquiring ^{17}O SSNMR spectra at the magnetic field of 21.1 T, we were able to establish the spectral signatures of various nonequivalent framework oxygen species present in the above-mentioned MOFs. The results presented in this report will serve as a benchmark for characterizing not only the existing MOFs but also the new MOF-based materials yet to come.

EXPERIMENTAL METHODS

^{17}O-Enriched MOF Preparations. *Zr-UiO-66.* In a typical synthesis of ^{17}O-enriched Zr-UiO-66, or $Zr_6O_4(OH)_4(BDC)_6$, 2.3 mmol of $ZrCl_4$ (Sigma-Aldrich 99.5%), 2.3 mmol of terephthalic acid (H_2BDC, 1,4-benzenedicarboxylic acid, Sigma-Aldrich, 98%), and 0.25 mL of ^{17}O-enriched water (CortecNet, 41.8% ^{17}O atom) were dissolved in 25 mL of *N,N′*-dimethylformamide (DMF, Reagent grade, Caledon). The solution was then added into a 30 mL Teflon-lined autoclave and heated at 473 K for 16 h. The product was recovered by vacuum filtration as a white powder.

MIL-53(Al)-lp and MIL-53(Al)-np. To prepare ^{17}O-enriched MIL-53(Al)-*lp*, or $Al(OH)(O_2C{-}C_6H_4{-}CO_2)\cdot(HO_2C{-}C_6H_4{-}CO_2H)_{0.7}$, 4.5 mmol of $Al(NO_3)_3\cdot 9H_2O$ (Sigma-Aldrich, 98%) and 5.9 mmol of terephthalic acid, both of which are solids, were first placed into a small Teflon cup. The cup was then put in a 23 mL Teflon-lined autoclave with 0.4 mL of ^{17}O-enriched H_2O (CortecNet, 41.8% ^{17}O atom) at the bottom (see Supporting Information Scheme S1 for the reaction vessel) and heated in an oven at 473 K for 3 days. The product was washed using deionized water and recovered by vacuum filtration to obtain a white powder. The powder was finally dried at 353 K for 12 h to get MIL-53(Al)-*lp*. MIL-53(Al)-*np* or $Al(OH)(O_2C{-}C_6H_4{-}CO_2)\cdot H_2O$ was prepared by calcining the MIL-53(Al)-*lp* at 603 K under dynamic vacuum for 3 days in air. The sample was slowly cooled to room temperature under vacuum and then sealed in a glass tube.

α-$Mg_3(HCOO)_6$. A typical synthesis of ^{17}O-enriched microporous α-$Mg_3(HCOO)_6$ involves mixing 3 mmol of $Mg(NO_3)_2\cdot 6H_2O$ (Sigma-Aldrich, 99%), 6 mmol of formic acid (Alfa Aesar, 97%), 0.25 g of ^{17}O-enriched H_2O (CortecNet, 41.8% ^{17}O atom), and 10 mL of DMF in a 23 mL Teflon-lined autoclave and then heated at 383 K for 2 days. The product was washed with DMF and recovered by vacuum filtration to obtain a white powder.

CPO-27-Mg. ^{17}O-enriched CPO-27-Mg was synthesized solvothermally. Typically, 0.75 mmol of 2,5-dihydroxyterephthalic acid (2,5-dioxido-1,4-benzenedicarboxylic acid, H_2DOBDC, Sigma-Aldrich, 98%) was first dissolved in a mixture of 0.25 g of ^{17}O-enriched H_2O (CortecNet, 41.8% ^{17}O atom), 3 mL of 1 M NaOH(aq), and 10 mL of tetrahydrofuran (THF) (Reagent grade, Caledon). The solution was then heated at 358 K for 12 h in a 23 mL Teflon-lined autoclave. This was followed by slowly adding 1.5 mmol of $Mg(NO_3)_2\cdot 6H_2O$ to the above solution. The resulting mixture was finally heated at 383 K for 3 days. The as-synthesized CPO-27-Mg was washed by THF and collected by vacuum filtration as a yellow powder. In order to obtain dehydrated CPO-27-Mg, the as-synthesized sample was exchanged with fresh methanol three times and activated under dynamic vacuum at 623 K overnight. The sample was allowed to cool gradually to room temperature under vacuum and sealed in a glass tube.

Powder X-ray Diffraction Measurements. The identity and purity of the ^{17}O-enriched MOFs were checked by powder XRD. Powder XRD patterns were recorded on a Rigaku diffractometer using Co Kα radiation (λ = 1.7902 Å). Samples were scanned at $5° \le 2\theta \le 65°$ at a scan rate of 10°/min with a step size of 0.02°. The patterns were converted to Cu Kα radiation (λ = 1.5405 Å) form to compare with the literature. The patterns (Figure S1) of the labeled MOFs are identical to those reported in the literature,[15,22,23,33] indicating that the products are phase pure.

^{17}O Solid-State NMR Spectroscopy. All ^{17}O SSNMR experiments were conducted at 21.1 T ($\nu_0(^{17}O)$ = 122.0 MHz) on a Bruker Avance II spectrometer at the National Ultrahigh-Field NMR Facility for Solids in Ottawa, Canada. The magic-angle spinning spectra were acquired by using the Hahn-echo pulse sequence with a 4 mm H/X MAS Bruker probe. The samples were packed in Si_3N_4 and ZrO_2 rotors for 10, 12, and 18 kHz MAS experiment. The pulse delay was 1−5 s. For selected samples, the MAS spectra were also obtained by using one-pulse sequence with a short excitation pulse, corresponding to a magnetization tip angle of less than 15° to ensure quantitative information on multiple sites in the samples. The pulse delay was 2 s. $^1H \rightarrow {}^{17}O$ cross-polarization (CP) experiments were also performed with contact time ranging from 0.2 to 10 ms. The ^{17}O chemical shifts were referenced to an external liquid sample of H_2O (δ_{iso} = 0 ppm). The liquid water sample was also used for rf power calibration. Typically, the nonselective $\pi/2$ pulse length is 12 μs, corresponding to a central transition selective $\pi/2$ pulse of 4 μs. More detailed spectrometer conditions used are listed in Table S1 of the Supporting Information. For Zr-UiO-66, MIL-53(Al)-*np*, and microporous α-$Mg_3(HCOO)_6$, ^{17}O SSNMR measurements were performed on the as-made samples. Sample packing was done in the atmospheric environment, and no precaution was needed. For dehydrated CPO-27-Mg and MIL-53(Al)-*lp*, the sample was packed into an airtight rotor in a glovebox under a nitrogen atmosphere to prevent sample from adsorbing water.

All ^{17}O NMR parameters, including quadrupolar coupling constants (C_Q), asymmetry parameters (η_Q), and isotropic chemical shifts (δ_{iso}), were determined by simulations of ^{17}O MAS spectra using the DMFIT program.[34] The experimental error for each measured parameter was determined by visual comparison of experimental spectra with simulations. The parameter of concern was varied bidirectionally starting from the best fit value and all other parameters were kept constant, until noticeable differences between the spectra were observed.

^{17}O SSNMR spectra of the MOFs were also acquired at 9.4 T on a Varian Infinity Plus 400 WB ($\nu_0(^{17}O)$ = 54.2 MHz) spectrometer. A Varian/Chemagnetics 5 mm HXY triple-tuned T3MAS probe was utilized for all MAS experiments (with proton decoupling), spinning at 10−11.5 kHz. Detailed experimental conditions are listed in Table S2, and the spectra are shown in Figure S2. For MIL-53(Al)-*lp*, MIL-53(Al)-*np*, and microporous α-$Mg_3(HCOO)_6$, although ^{17}O signals were observed, the signals from different ^{17}O sites overlap with each

other and with spinning sidebands as well due to the limitation of the spinning speed which can be achieved. For CPO-27, no signal was observed after 22 h, which is consistent with the fact that this particular sample has the lowest degree of ^{17}O-enrichment. In the spectrum of Zr-UiO-66, the signal of carboxylate oxygen appears to be missing. Overall, the factors such as the low sensitivity and the larger quadrupolar broadening at lower field strength as well as the low spinning rates limited by the probe available to us make the ^{17}O spectra acquired at 9.4 T not suitable for analysis. Therefore, they will not be discussed further.

Theoretical Calculations. Gauge including projector augmented wave (GIPAW) quantum chemical calculations[35,36] were conducted using the CASTEP code (version 4.4, Accelrys Materials Studio). The NMR module was used to calculate the ^{17}O NMR parameters. Unit cell parameters and atomic coordinates were taken from the crystal structures of the MOFs examined.[15,22,23,33] When necessary, the geometry optimization was performed. The unit cell parameters were not allowed to change since the unit cell dimensions are well-defined from the powder XRD. The solvent/guest molecules were kept in the pores whenever possible. The calculations were performed using ultrasoft pseudopotentials generated from the "on-the-fly" method implemented within the CASTEP. The generalized gradient approximation (GGA) with Perdew, Burke, and Ernzerhof (PBE) functional was used. The $C_Q(^{17}O)$ values were calculated from the EFG tensor produced by the CASTEP calculation using $Q(^{17}O) = -2.558 \times 10^{-30}$ m^2.[37] The isotropic chemical shift for ^{17}O was computed using the correlation $\delta_{iso} = 287.5 - \sigma_{iso}$ (all in ppm), where 287.5 ppm is the absolute shielding value of liquid H_2O ($\delta_{iso} = 0$ ppm).[38]

RESULTS AND DISCUSSION

As mentioned earlier, the major obstacles that preventing ^{17}O SSNMR from being used for MOF characterization are the synthetic effort in ^{17}O isotopic enrichment and the associated cost. In this work, depending on the target MOF system, several strategies were used to cost-effectively prepare ^{17}O-enriched MOFs, which are briefly described below. More details are provided in the Experimental Methods section.

(1) A recent study reported that ^{17}O-enriched oxides can be economically prepared ionothermally with ionic liquid incorporating a trace amount of ^{17}O-enriched water as solvent.[39] Since many MOFs are synthesized using nonaqueous solvents in the presence of a very small amount of water, such situation can also be exploited for making ^{17}O-enriched MOFs effectively. Indeed, we prepared MOF Zr-UiO-66, or $Zr_6O_4(OH)_4(BDC)_6$, by directly reacting solid $ZrCl_4$ and terephthalic acid in 25 mL of DMF with only 0.25 mL of ^{17}O-enriched water. ^{17}O-enriched microporous α-magnesium formate, α-$Mg_3(HCOO)_6$, was also prepared using the same approach.

(2) MOFs are often prepared under hydrothermal synthesis (HTS) conditions using water as solvent. For the MOFs made by HTS, we can use "dry gel conversion" (DGC) method, a technique that is used as an alternative approach to hydrothermal method for the synthesis of zeolites.[40] It involves treating predried gel powder (containing the sources of framework elements and structure directing agent) with vapor generated by heating a very small amount of water at elevated temperature in an autoclave. Such method has been used earlier to prepare ^{17}O-enriched $AlPO_4$-based molecular sieves.[41] In the present case, we prepared ^{17}O-enriched MIL-53(Al) by simply putting Al-$(NO_3)_3{\cdot}9H_2O$ and terephthalic acid solids inside a small Teflon cup placed in a Teflon-lined autoclave with 0.4 g of ^{17}O enriched water at the bottom of the autoclave (Scheme S1). The solids and ^{17}O-enriched water are never physically in contact before heating. Heating of the autoclave at 473 K for 3 days results in highly crystalline MIL-53(Al). Since many MOFs can be prepared by DGC methods, this approach can be widely used for ^{17}O enrichment.

(3) The third method is similar to that used for incorporating ^{17}O into MOF-5.[29] It involves direct ^{17}O-exchange of carboxylate and phenol oxygens with ^{17}O-enriched water in NaOH solution prior to the addition of metal ions. A similar approach was also used in this work to prepare ^{17}O-enriched CPO-27-Mg.

Estimation of the degree of ^{17}O-enrichment in MOFs was a challenging task as these MOFs do not dissolve in solvents. We established a protocol to evaluate ^{17}O-enrichment in MOFs by using time-of-flight secondary ion mass spectrometry (TOF-SIMS). The $^{17}O/^{16}O$ isotope ratios estimated for the four ^{17}O-enriched samples of $Mg_3(HCOO)_6$, MIL-53-(Al), Zr-UiO-66, and CPO-27-Mg are 8.2 ± 0.2%, 5.8 ± 0.1%, 2.4 ± 0.2%, and 1.5 ± 0.1%, respectively. When comparing with the $^{17}O/^{16}O$ ratio of 0.0381% at natural abundance, the degrees of the enrichment are estimated at 215, 152, 63, and 39 times the natural abundance of ^{17}O for $Mg_3(HCOO)_6$, MIL-53-(Al), Zr-UiO-66, and CPO-27-Mg, respectively. Note that Zr-UiO-66 used was the as-synthesized sample with solvent DMF and a small amount of water which are not ^{17}O labeled. Using the TGA data, the $^{17}O/^{16}O$ ratio in the framework was adjusted to be 3.38%, corresponding to 88 times of the natural abundance of ^{17}O. See the Supporting Information for the experimental procedure and data analyses.

The ^{17}O magic-angle spinning (MAS) spectra of the above-prepared ^{17}O-enriched MOFs were acquired at a magnetic field of 21.1 T. The spectra are sensitive to the oxygen bonding mode to the metal center and can be used to distinguish chemically different oxygen species and, under favorable conditions, the crystallographically nonequivalent oxygen sites.

MOF Zr-UiO-66 is used here as an example to demonstrate that chemically different oxygen species, which are difficult to distinguish by X-ray diffraction, can be straightforwardly differentiated by ^{17}O SSNMR. Zr-UiO-66 is a MOF with exceptionally high thermal stability.[22] The reported crystal structure of Zr-UiO-66 was determined from the powder XRD data.[22] Its structure is built upon from the polyhedra containing eight-coordinated zirconium atoms, which are connected by 1,4-BDC (1,4-benzenedicarboxylate) linkers (Figure 1). The basic building unit, $Zr_6O_4(OH)_4$(1,4-BDC)$_6$, consists of an octahedral core formed by six Zr atoms. There are three chemically nonequivalent oxygen species associated with each $Zr_6O_4(OH)_4$(1,4-BDC)$_6$ unit (Figure 1): (1) the oxygen atoms from carboxylate group; (2) four μ_3-O^{2-} anions capped alternatively on the four of the eight triangular faces of the octahedron; (3) four μ_3-OH groups capped on the remaining triangular faces. Since the two capping species are difficult to differentiate by X-ray diffraction, the existing evidence for μ_3-

dx.doi.org/10.1021/jp403512m | J. Phys. Chem. C 2013, 117, 16953−16960

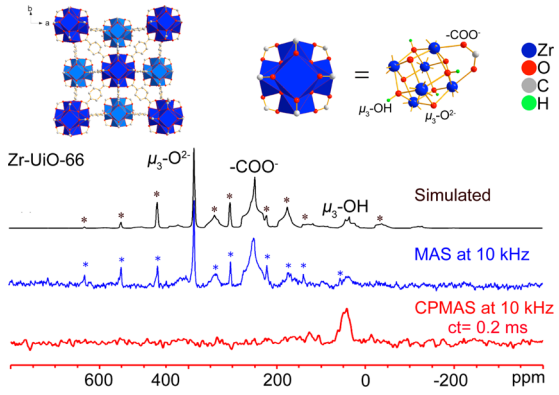

Figure 1. Illustrations of the framework (top left), the metal coordination environment (top right),[22] and ^{17}O MAS and CP-MAS NMR spectra of Zr-UiO-66. *: spinning sidebands.

OH groups initially comes from IR spectroscopy.[42] As shown below, these two capping species can be easily differentiated by ^{17}O MAS SSNMR. Figure 1 displays the ^{17}O MAS spectrum of as-synthesized Zr-UiO-66 spun at 10 kHz acquired at the field strength of 21.1 T. There are three distinct signals in the spectrum. For the broad peak at around 270 ppm, the spectral simulation (Figure 1) reveals the following NMR parameters (Table 1): C_Q = 7.1 MHz, η_Q = 0.85, δ_{iso} = 278 ppm. Since the

Table 1. Experimental ^{17}O NMR Parameters of the MOF Samples

sample	O site	$\lvert C_Q \rvert$ (MHz)	η_Q	δ_{iso} (ppm)
Zr-UiO-66	$-COO^-$	7.1(3)	0.85(10)	278(10)
	μ_3-O^{2-}	2.0(3)	0.50(10)	386(10)
	μ_3-OH	6.5(3)	0.60(10)	65(10)
MIL-53(Al)-*lp*	μ_2-OH	6.1(3)	0.60(10)	22(10)
	$-COO^-$	7.9(3)	0.58(10)	232(10)
MIL-53(Al)-*np*	μ_2-OH	6.5(3)	0.85(10)	24(10)
	$-COO^-$ site 1	6.9(3)	0.85(10)	256(10)
	$-COO^-$ site 2	5.5(3)	0.85(10)	206(10)
	H_2O	2.5(10)	0	−12(5)
α-$Mg_3(HCOO)_6$	O site 1	6.8(3)	0.80(10)	230(5)
	O site 2	8.0(3)	0.45(10)	289(5)
CPO-27-Mg	Ph−O^-	9.1(3)	0.60(10)	87(10)
	μ_2-COO^-	7.3(3)	0.10(10)	226(10)
	μ_1-COO^-	7.1(3)	0.70(10)	251(10)

chemical shift and the C_Q value are consistent with the carboxylate oxygens reported in the literature,[25,26] this peak is assigned to the carboxylate oxygen in 1,4-BDC ligands. The resonance appearing at 65 ppm is assigned to the capping μ_3-OH. The identity of this resonance is further confirmed by performing ^{1}H → ^{17}O cross-polarization (CP) experiment with a short contact time (ct) of 0.2 ms under the MAS conditions. CP is mediated by the heteronuclear dipolar interaction. At a very short contact time, only the ^{17}O with proton in its close proximity will be observed. Thus, seeing the 65 ppm peak in the CP-MAS spectrum (Figure 1) is direct evidence that this resonance originates from μ_3-OH species. The third signal is a very sharp line at 386 ppm. Based on its chemical shift, this peak is assigned to the capping μ_3-O^{2-} species.[43]

One striking feature of many MOFs is that they exhibit an unusually large degree of framework flexibility.[44,45] For these MOFs, adsorption of certain guest molecules can induce a very large change in unit cell volume. The unit cell expansion/contraction does not usually result in the breaking of the chemical bonds holding the framework in place. A phase transformation, however, often occurs concomitantly. Using MIL-53(Al), a typical flexible MOF, we show that the phase transition can be detected by ^{17}O SSNMR. The basic building unit of MIL-53(Al) is an $AlO_4(\mu_2\text{-}OH)_2$ octahedron (Figure 2).[15] Al is equatorially bound to four oxygen atoms in

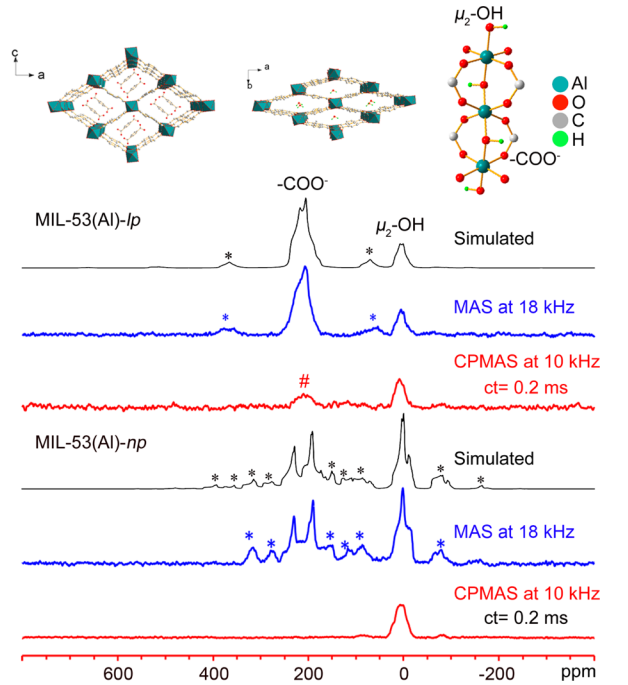

Figure 2. Illustrations of the frameworks of MIL-53(Al)-*lp* (top left) and MIL-53(Al)-*np* (top middle), the metal coordination environment (top right),[15] and ^{17}O NMR spectra of MIL-53(Al). #: unreacted 1,4-benzenedicarboxylic acid. *: spinning sidebands.

carboxylate groups from four (1,4-BDC) linkers. The $AlO_4(\mu_2\text{-}OH)_2$ octahedra are linked via two μ_2-hydroxo (μ_2-OH) groups (*trans* to each other) to form infinite chains along the *b* direction. The chains are connected via 1,4-BDC linkers to form a 1D channel system. As-synthesized sample crystallizes in an orthorhombic phase (also called the large pore (*lp*) phase). Upon removing the unreacted terephthalic acid from the channels at high temperature and subsequently adsorption of water, the orthorhombic phase transforms to a monoclinic phase with a much smaller channel dimensions (therefore, it is also referred to as the narrow pore (*np*) phase).[15]

The framework structure of the as-synthesized MIL-53(Al)-*lp* was determined from powder X-ray diffraction data.[15] The existence of μ_2-hydroxo (OH) groups was proposed based on ^{1}H MAS NMR spectrum where a broad weak shoulder at 2.9 ppm was assigned to the hydrogen in μ_2-OH group.[15] The ^{17}O MAS spectrum of the as-synthesized MIL-53(Al) is illustrated in Figure 2 in which two groups of signals are seen clearly. The strong resonance at about 230 ppm are assigned to the oxygen atoms in the 1,4-BDC linkers. Based on the previous ^{17}O NMR work on aluminum oxides, the weaker signal at around 20 ppm is due to either the bridging oxygen in the Al−OH−Al group as proposed in the literature or the oxygen in an Al−O−Al linkage.[46] To clarify the situation, we further carried out ^{1}H → ^{17}O CP-MAS experiments with different contact times (Figure

dx.doi.org/10.1021/jp403512m | J. Phys. Chem. C 2013, 117, 16953−16960

2 and Figure S3). Seeing a strong CP signal at very short contact times confirms that this signal originates from the oxygen in the Al−OH−Al unit. The weak signal (labeled with #) in the CP-MAS spectrum is from the CO^{17}OH group of unreacted terephthalic acid occluded inside the pore. Spectral simulations (Figure 2) yielded the NMR parameters of the oxygen species (Table 1). The crystal structure of as-synthesized MIL-53(Al)-*lp* indicates that there are two crystallographically nonequivalent carboxylate oxygen sites.[15] Attempt was made to separate these two sites by performing ^{17}O triple-quantum MAS (3QMAS) experiment[47] at 21.1 T (spectrum not shown). Unfortunately, after 24 h, the resolution in the indirect dimension is still insufficient to resolve signals from individual oxygen sites due to t_1 noise originating from poor sensitivity. Perhaps, a material with a higher degree of enrichment is needed. We also carried out GIPAW DFT calculations. The results predicted that these two crystallographically nonequivalent carboxylate oxygen sites have almost identical C_Q, η_Q, and δ_{iso} (Table S3).

As mentioned earlier, MIL-53(Al)-*lp* undergoes a phase transition from an orthorhombic to a monoclinic phase upon calcination and subsequent water adsorption.[15] Such transformation is accompanied by one-third reduction in the unit cell volume without breaking chemical bonds. This phase transition has been investigated earlier by ^{1}H, ^{13}C, ^{27}Al,[15] and ^{129}Xe[12] NMR. For example, it was shown that upon transformation from *lp* to *np*, the C_Q(^{27}Al) increased from 7.60 to 10.67 MHz.[15] Here, we demonstrated that the *lp* to *np* phase change can also be detected by ^{17}O SSNMR. Figure 2 displays the ^{17}O MAS spectrum of the *np* phase of MIL-53(Al) with water as guest species. It looks distinctly different from that of the *lp* phase. Specifically, the strong peak due to the framework carboxylate oxygen now split into several resonances, which is indicative of the lowering of the crystal symmetry. Similar to the *lp* phase, the peak at around 20 ppm is assigned to the μ_2-OH group overlapping with a sharp signal from the water molecules trapped in the channel. This assignment is consistent with the CP-MAS spectrum with a short ct = 0.2 ms, where the intensity of the sharp resonance from water disappeared owning to the fact that the mobility of water reduces the CP efficiency. It is also noticed that since the unreacted terephthalic acid is removed in the *np* phase, the CP signal originating from the COOH group in the unreacted terephthalic acid observed in the as-synthesized phase no longer appears in the CP spectrum of the *np* phase. Taking all the information into consideration, the MAS spectrum can be fitted with four oxygen sites (two crystallographically nonequivalent carboxylate oxygens, one μ_2-OH group and one from water molecules). The simulated spectra are shown in Figure 2. The NMR parameters extracted from simulations are summarized in Table 1. The proposed crystal structure suggests that there are four unique carboxylate oxygens. The CASTEP calculations using optimized geometry show that O2 and O2b have very similar C_Q and δ_{iso}; the same is true for O3 and O3b. The calculated η_Q values are very similar for all four sites. On the basis of the CASTEP calculations (Table S3), we can assign the observed signal at 206 ppm to O2 and O2b, whereas the resonance at 256 ppm to O3 and O3b. This example shows that under favorable conditions the change in the number of crystallographically nonequivalent oxygens due to phase transition can be followed by ^{17}O SSNMR.

Microporous α-magnesium formate, α-$Mg_3(HCOO)_6$, represents the situation where one of the oxygen in carboxylate group is bonded to one metal center (μ_1-O) and the other oxygen in the same $-COO^-$ group bound to two metal ions (μ_2-O). α-$Mg_3(HCOO)_6$ was first prepared by Rood and coworkers[33] and is one of the successfully commercialized MOFs.[48,49] Its basic building unit is a MgO_6 octahedron with each Mg cation bound to six oxygens from six formate anions ($HCOO^-$). The framework consists of corner- and edge-sharing MgO_6 octahedra with one-dimensional channel systems (4.5 × 5.5 Å^2) along the *b* direction (Figure 3). The ^{17}O MAS

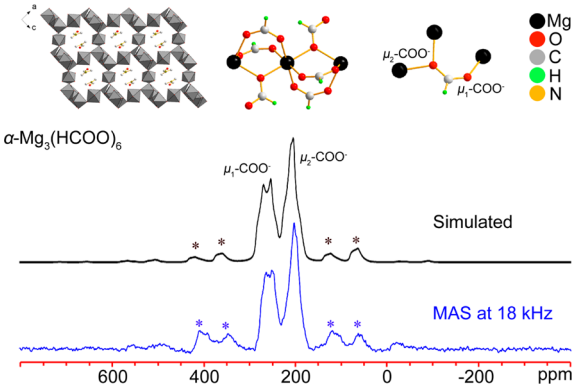

Figure 3. Illustrations of the framework with DMF (solvent) in the pore, Mg, and oxygen coordination environments[33] and ^{17}O NMR spectra of α-$Mg_3(HCOO)_6$. *: spinning sidebands.

spectrum of the as-synthesized α-$Mg_3(HCOO)_6$ spun at 18 kHz acquired at the field strength of 21.1 T is shown in Figure 3. It contains two separate resonances. The spectral simulations (Figure 3) yielded the following NMR parameters (Table 1): site 1: C_Q = 6.8 MHz, η_Q = 0.80, δ_{iso} = 230 ppm; site 2: C_Q = 8.0 MHz, η_Q = 0.45, δ_{iso} = 289 ppm. The chemical shifts and the C_Q values are in the range of carboxylate oxygen reported in the literature.[25,26] Thus, the ^{17}O MAS spectrum clearly shows that there are at least two groups of nonequivalent oxygens from the formate anions. The crystal structure indicates that there are 12 nonequivalent oxygen sites. They can be further divided into two groups based on their bonding modes. Six independent oxygens adopt μ_2-O bonding mode, whereas the other six crystallographically nonequivalent O sites adopt μ_1-O mode. It appears that the two observed resonances originate from μ_2-O and μ_1-O oxygens. To confirm this argument and further assign the signals, GIPAW DFT calculations were carried out, and the results (Table S3) clearly show that six μ_2-oxygens have very similar EFG parameters and chemical shifts (C_Q = 5.96−6.82 MHz; η_Q = 0.74−0.93, δ_{iso} = 210.3−234.0 ppm) and that the NMR parameters of the six μ_1-oxygens are akin to each other (C_Q = 7.92−8.07 MHz; η_Q = 0.19−0.24, δ_{iso} = 275.8−292.0 ppm). Thus, we can assign the signals at 230 and 289 ppm to the six μ_2- and the six μ_1-oxygens, respectively. This sample also illustrates why we had to carry out the MAS experiment at a very high magnetic field as it is evident from Figure 3 that the peaks due to different bonding modes are barely resolved even at 21.1 T. For each bonding mode, the local environments of six crystallographically nonequivalent oxygen sites are so close that we were not able to distinguish them further due to their very similar NMR parameters. To separate these sites with close environments, perhaps in future resolution-enhancement techniques including double-rotation (DOR),[50,51] multiple-quantum MAS (MQMAS),[47] and the satellite transition MAS (STMAS)[52] should be used. They can

dx.doi.org/10.1021/jp403512m | J. Phys. Chem. C 2013, 117, 16953−16960

also be combined with sensitivity-enhancement method such as DNP.[53]

CPO-27-Mg is another Mg-containing MOF with potential industrial applications due to its exceptional ability of adsorbing CO_2.[31] The precursor of the organic linker is 2,5-dioxido-1,4-benzenedicarboxylic acid which contains two phenol and two carboxylic groups. Upon deprotonation, oxygens from all four groups in the same linker are bound to the Mg atoms to form a honeycomb structure with a one-dimensional channel system (Figure 4). As-synthesized phase contains MgO_6 octahedra

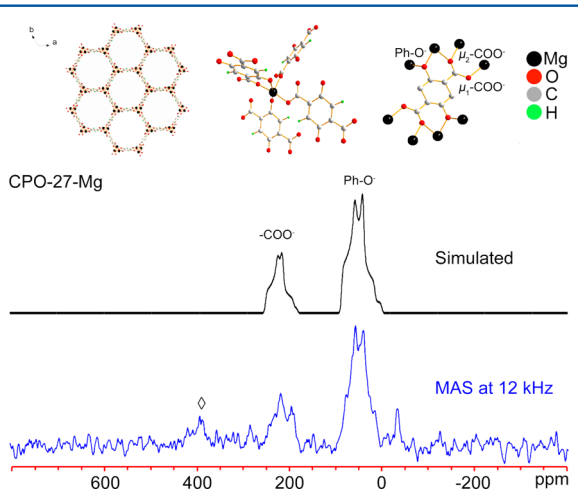

Figure 4. Illustrations of the framework, Mg and oxygen coordination environments[23] and ^{17}O NMR spectra of CPO-27-Mg. *: spinning sidebands. ◊: ^{17}O background signal from ZrO_2 rotor.[55]

with each metal ion bound to five oxygens from four 2,5-dioxido-1,4-benzenedicarboxylate (DOBDC).[23] The sixth coordination site is occupied by a water molecule, which can be removed upon dehydration. The ^{17}O MAS spectrum of as-synthesized CPO-27-Mg is overwhelmingly dominated by a broad peak with Gaussian shape centered at around 0 ppm (spectrum not shown). This very strong peak is due to the large amount of water molecules occluded inside the channels. In order to clearly observe carboxylate and phenol oxygens, we examined the dehydrated phase. Its ^{17}O MAS spectrum is illustrated in Figure 4, which contains several resonances. The peak centered at around 80 ppm is due to the phenol oxygen bound to the Mg ions based on the shift value.[25,26] The signal at about 230 ppm is assigned to the framework carboxylate oxygen. We noticed that the intensity of the carboxylate oxygens is much weaker than that of the phenol oxygen. We further obtained a MAS spectrum by using a much longer pulse delay of 20 s (spectrum not shown) which indicates that the difference in intensity is not due to spin−lattice relaxation time (T_1). It is likely that during the synthesis the phenol oxygen undergoes a much faster exchange with ^{17}O in water. There is a small sharp feature at about −20 ppm which might be due to the Mg−OH formed during the dehydration process.[54]

CONCLUSIONS

In this work, we successfully prepared several prototypical ^{17}O-enriched MOFs. Because of the diversity of MOF-based materials, different types of MOFs may require different isotopic enrichment methods to effectively incorporate ^{17}O from ^{17}O-enriched H_2O. Several synthetic strategies for ^{17}O-enrichment were discussed. Using these ^{17}O-enriched MOFs, we were able to acquire ^{17}O SSNMR spectra at a magnetic field of 21.1 T. They provide distinct spectral signatures of various key oxygen species commonly existing in representative MOFs. We demonstrate that ^{17}O SSNMR can be used to differentiate chemically and, under favorite circumstances, crystallographically nonequivalent oxygens and to follow the phase transitions. The synthetic approaches for preparation of ^{17}O-enriched sample described in this paper are fairly simple and cost-effective. It is hoped that this work will encourage other researchers to use ^{17}O SSNMR for MOF characterization.

ASSOCIATED CONTENT

Supporting Information

Calculated ^{17}O NMR parameters, schematic description of the reaction vessel, powder XRD patterns, ^{17}O MAS NMR spectra acquired at 9.4 T, ^{17}O CP MAS spectra of MIL-53(Al)-*lp* at 21.1 T, detailed spectrometer conditions used, and the procedure for ^{17}O enrichment analysis. This material is available free of charge via the Internet at http://pubs.acs.org.

AUTHOR INFORMATION

Corresponding Author

*Tel (519) 661-2111, ext. 86384; e-mail yhuang@uwo.ca (Y.H.).

Notes

The authors declare no competing financial interest.

ACKNOWLEDGMENTS

Y.H. thanks the Natural Science and Engineering Research Council (NSERC) of Canada for a Discovery grant and a DAS award. Funding from the Canada Research Chair program is also gratefully acknowledged. The NSERC is also acknowledged for a Major Resource Support grant. We thank The University of Western Ontario for a small ADF grant. Access to the 900 MHz NMR spectrometer and the CASTEP software was provided by the National Ultrahigh Field NMR Facility for Solids (Ottawa, Canada), a national research facility funded by the Canada Foundation for Innovation, the Ontario Innovation Trust, Recherche Québec, the National Research Council Canada, and Bruker BioSpin and managed by the University of Ottawa.

REFERENCES

(1) Special Issue for Metal-Organic Frameworks: Zhou, H.-C.; Long, J. R.; Yaghi, O. M. *Chem. Rev.* **2012**, *112*, 673−1268.

(2) Sutrisno, A.; Huang, Y. Solid-State NMR: A Powerful Tool for Characterization of Metal-Organic Frameworks. *Solid State Nucl. Magn. Reson.* **2013**, *49*−*50*, 1−11.

(3) Hoffmann, H. C.; Debowski, M.; Mueller, P.; Paasch, S.; Senkovska, I.; Kaskel, S.; Brunner, E. Solid-State NMR Spectroscopy of Metal-Organic Framework Compounds (MOFs). *Materials* **2012**, *5*, 2537−2572.

(4) Dawson, D. M.; Jamieson, L. E.; Mohideen, M. I. H.; McKinlay, A. C.; Smellie, I. A.; Cadou, R.; Keddie, N. S.; Morris, R. E.; Ashbrook, S. E. High-Resolution Solid-State ^{13}C NMR Spectroscopy of the Paramagnetic Metal-Organic Frameworks, STAM-1 and HKUST-1. *Phys. Chem. Chem. Phys.* **2013**, *15*, 919−929.

(5) Besara, T.; Jain, P.; Dalal, N. S.; Kuhns, P. L.; Reyes, A. P.; Kroto, H. W.; Cheetham, A. K. Mechanism of the Order-Disorder Phase Transition, and Glassy Behavior in the Metal-Organic Framework $[(CH_3)_2NH_2]Zn(HCOO)_3$. *Proc. Natl. Acad. Sci. U. S. A.* **2011**, *108*, 6828−6832.

(6) Gul-E-Noor, F.; Jee, B.; Mendt, M.; Himsl, D.; Poeppl, A.; Hartmann, M.; Haase, J.; Krautscheid, H.; Bertmer, M. Formation of

Mixed Metal $Cu_{3-x}Zn_x(btc)_2$ Frameworks with Different Zinc Contents: Incorporation of Zn^{2+} into the Metal-Organic Framework Structure as Studied by Solid-State NMR. *J. Phys. Chem. C* **2012**, *116*, 20866−20873.
(7) Jiang, Y.; Huang, J.; Marx, S.; Kleist, W.; Hunger, M.; Baiker, A. Effect of Dehydration on the Local Structure of Framework Aluminum Atoms in Mixed Linker MIL-53(Al) Materials Studied by Solid-State NMR Spectroscopy. *J. Phys. Chem. Lett.* **2010**, *1*, 2886−2890.
(8) Devautour-Vinot, S.; Maurin, G.; Serre, C.; Horcajada, P.; Paula da Cunha, D.; Guillerm, V.; de Souza Costa, E.; Taulelle, F.; Martineau, C. Structure and Dynamics of the Functionalized MOF Type UiO-66(Zr): NMR and Dielectric Relaxation Spectroscopies Coupled with DFT Calculations. *Chem. Mater.* **2012**, *24*, 2168−2177.
(9) Kolokolov, D. I.; Stepanov, A. G.; Guillerm, V.; Serre, C.; Frick, B.; Jobic, H. Probing the Dynamics of the Porous Zr Terephthalate UiO-66 Framework Using ^{2}H NMR and Neutron Scattering. *J. Phys. Chem. C* **2012**, *116*, 12131−12136.
(10) Shustova, N. B.; Ong, T.-C.; Cozzolino, A. F.; Michaelis, V. K.; Griffin, R. G.; Dinca, M. Phenyl Ring Dynamics in a Tetraphenylethylene-Bridged Metal-Organic Framework: Implications for the Mechanism of Aggregation-Induced Emission. *J. Am. Chem. Soc.* **2012**, *134*, 15061−15070.
(11) Pawsey, S.; Moudrakovski, I.; Ripmeester, J.; Wang, L.-Q.; Exarhos, G. J.; Rowsell, J. L. C.; Yaghi, O. M. Hyperpolarized ^{129}Xe Nuclear Magnetic Resonance Studies of Isoreticular Metal-Organic Frameworks. *J. Phys. Chem. C* **2007**, *111*, 6060−6067.
(12) Springuel-Huet, M.-A.; Nossov, A.; Adem, Z.; Guenneau, F.; Volkringer, C.; Loiseau, T.; Ferey, G.; Gedeon, A. ^{129}Xe NMR Study of the Framework Flexibility of the Porous Hybrid MIL-53(Al). *J. Am. Chem. Soc.* **2010**, *132*, 11599−11607.
(13) Ooms, K. J.; Wasylishen, R. E. ^{129}Xe NMR Study of Xenon in Iso-Reticular Metal-Organic Frameworks. *Microporous Mesoporous Mater.* **2007**, *103*, 341−351.
(14) Rossini, A. J.; Zagdoun, A.; Lelli, M.; Canivet, J.; Aguado, S.; Ouari, O.; Tordo, P.; Rosay, M.; Maas, W. E.; Coperet, C.; Farrusseng, D.; Emsley, L.; Lesage, A. Dynamic Nuclear Polarization Enhanced Solid-State NMR Spectroscopy of Functionalized Metal-Organic Frameworks. *Angew. Chem., Int. Ed.* **2012**, *51*, 123−127.
(15) Loiseau, T.; Serre, C.; Huguenard, C.; Fink, G.; Taulelle, F.; Henry, M.; Bataille, T.; Ferey, G. A Rationale for the Large Breathing of the Porous Aluminum Terephthalate (MIL-53) upon Hydration. *Chem.—Eur. J.* **2004**, *10*, 1373−1382.
(16) Loiseau, T.; Lecroq, L.; Volkringer, C.; Marrot, J.; Ferey, G.; Haouas, M.; Taulelle, F.; Bourrelly, S.; Llewellyn, P. L.; Latroche, M. MIL-96, a Porous Aluminum Trimesate 3D Structure Constructed from a Hexagonal Network of 18-Membered Rings and μ_3-Oxo-Centered Trinuclear Units. *J. Am. Chem. Soc.* **2006**, *128*, 10223−10230.
(17) Mowat, J. P. S.; Miller, S. R.; Slawin, A. M. Z.; Seymour, V. R.; Ashbrook, S. E.; Wright, P. A. Synthesis, Characterization and Adsorption Properties of Microporous Scandium Carboxylates with Rigid and Flexible Frameworks. *Microporous Mesoporous Mater.* **2011**, *142*, 322−333.
(18) Hajjar, R.; Volkringer, C.; Loiseau, T.; Guillou, N.; Marrot, J.; Ferey, G.; Margiolaki, I.; Fink, G.; Morais, C.; Taulelle, F. ^{71}Ga Slow-CTMAS NMR and Crystal Structures of MOF-Type Gallium Carboxylates with Infinite Edge-Sharing Octahedra Chains (MIL-120 and MIL-124). *Chem. Mater.* **2011**, *23*, 39−47.
(19) Xu, J.; Terskikh, V. V.; Huang, Y. ^{25}Mg Solid-State NMR: A Sensitive Probe of Adsorbing Guest Molecules on a Metal Center in Metal-Organic Framework CPO-27-Mg. *J. Phys. Chem. Lett.* **2013**, *4*, 7−11.
(20) Xu, J.; Terskikh, V. V.; Huang, Y. Resolving Multiple Non-equivalent Metal Sites in Magnesium-Containing Metal−Organic Frameworks by Natural Abundance ^{25}Mg Solid-State NMR Spectroscopy. *Chem.—Eur. J.* **2013**, *19*, 4432−4436.
(21) Sutrisno, A.; Terskikh, V. V.; Shi, Q.; Song, Z.; Dong, J.; Ding, S. Y.; Wang, W.; Provost, B. R.; Daff, T. D.; Woo, T. K.; Huang, Y. Characterization of Zn-Containing Metal-Organic Frameworks by Solid-State ^{67}Zn NMR Spectroscopy and Computational Modeling. *Chem.—Eur. J.* **2012**, *18*, 12251−12259.
(22) Hafizovic Cavka, J.; Jakobsen, S.; Olsbye, U.; Guillou, N.; Lamberti, C.; Bordiga, S.; Lillerud, K. P. A New Zirconium Inorganic Building Brick Forming Metal Organic Frameworks with Exceptional Stability. *J. Am. Chem. Soc.* **2008**, *130*, 13850−13851.
(23) Dietzel, P. D. C.; Blom, R.; Fjellvaag, H. Base-Induced Formation of Two Magnesium Metal-Organic Framework Compounds with a Bifunctional Tetratopic Ligand. *Eur. J. Inorg. Chem.* **2008**, *2008*, 3624−3632.
(24) Ashbrook, S. E.; Smith, M. E. Solid State ^{17}O NMR - An Introduction to the Background Principles and Applications to Inorganic Materials. *Chem. Soc. Rev.* **2006**, *35*, 718−735.
(25) Wu, G. Solid-State ^{17}O NMR Studies of Organic and Biological Molecules. *Prog. Nucl. Magn. Reson. Spectrosc.* **2008**, *52*, 118−169.
(26) Gerothanassis, I. P. Oxygen-17 NMR Spectroscopy: Basic Principles and Applications (Part I). *Prog. Nucl. Magn. Reson. Spectrosc.* **2010**, *56*, 95−197.
(27) Bonhomme, C.; Coelho, C.; Baccile, N.; Gervais, C.; Azais, T.; Babonneau, F. Advanced Solid State NMR Techniques for the Characterization of Sol-Gel-Derived Materials. *Acc. Chem. Res.* **2007**, *40*, 738−746.
(28) Yamada, K. Recent Applications of Solid-State ^{17}O NMR. *Annu. Rep. NMR Spectrosc.* **2010**, *70*, 115−158.
(29) Mueller, M.; Hermes, S.; Kaehler, K.; van den Berg, M. W. E.; Muhler, M.; Fischer, R. A. Loading of MOF-5 with Cu and ZnO Nanoparticles by Gas-Phase Infiltration with Organometallic Precursors: Properties of Cu/ZnO@MOF-5 as Catalyst for Methanol Synthesis. *Chem. Mater.* **2008**, *20*, 4576−4587.
(30) Rosi, N. L.; Kim, J.; Eddaoudi, M.; Chen, B.; O'Keeffe, M.; Yaghi, O. M. Rod Packings and Metal-Organic Frameworks Constructed from Rod-Shaped Secondary Building Units. *J. Am. Chem. Soc.* **2005**, *127*, 1504−1518.
(31) Caskey, S. R.; Wong-Foy, A. G.; Matzger, A. J. Dramatic Tuning of Carbon Dioxide Uptake via Metal Substitution in a Coordination Polymer with Cylindrical Pores. *J. Am. Chem. Soc.* **2008**, *130*, 10870−10871.
(32) McDonald, T. M.; Lee, W. R.; Mason, J. A.; Wiers, B. M.; Hong, C. S.; Long, J. R. Capture of Carbon Dioxide from Air and Flue Gas in the Alkylamine-Appended Metal-Organic Framework mmen-Mg_2(dobpdc). *J. Am. Chem. Soc.* **2012**, *134*, 7056−7065.
(33) Rood, J. A.; Noll, B. C.; Henderson, K. W. Synthesis, Structural Characterization, Gas Sorption and Guest-Exchange Studies of the Lightweight, Porous Metal-Organic Framework α-$[Mg_3(O_2CH)_6]$. *Inorg. Chem.* **2006**, *45*, 5521−5528.
(34) Massiot, D.; Fayon, F.; Capron, M.; King, I.; Le Calve, S.; Alonso, B.; Durand, J.-O.; Bujoli, B.; Gan, Z.; Hoatson, G. Modeling One- and Two-Dimensional Solid-State NMR Spectra. *Magn. Reson. Chem.* **2002**, *40*, 70−76.
(35) Charpentier, T. The PAW/GIPAW Approach for Computing NMR Parameters: A New Dimension Added to NMR Study of Solids. *Solid State Nucl. Magn. Reson.* **2011**, *40*, 1−20.
(36) Bonhomme, C.; Gervais, C.; Babonneau, F.; Coelho, C.; Pourpoint, F.; Azais, T.; Ashbrook, S. E.; Griffin, J. M.; Yates, J. R.; Mauri, F.; Pickard, C. J. First-Principles Calculation of NMR Parameters Using the Gauge Including Projector Augmented Wave Method: A Chemist's Point of View. *Chem. Rev.* **2012**, *112*, 5733−5779.
(37) Pyykko, P. Year-2008 Nuclear Quadrupole Moments. *Mol. Phys.* **2008**, *106*, 1965−1974.
(38) Wasylishen, R. E.; Bryce, D. L. A Revised Experimental Absolute Magnetic Shielding Scale for Oxygen. *J. Chem. Phys.* **2002**, *117*, 10061−10066.
(39) Griffin, J. M.; Clark, L.; Seymour, V. R.; Aldous, D. W.; Dawson, D. M.; Iuga, D.; Morris, R. E.; Ashbrook, S. E. Ionothermal ^{17}O Enrichment of Oxides Using Microlitre Quantities of Labelled Water. *Chem. Sci.* **2012**, *3*, 2293−2300.

(40) Xu, W.; Dong, J.; Li, J.; Li, J.; Wu, F. A Novel Method for the Preparation of Zeolite ZSM-5. *J. Chem. Soc., Chem. Commun.* **1990**, 755−756.
(41) Chen, B.; Huang, Y. ^{17}O Solid-State NMR Spectroscopic Studies of the Involvement of Water Vapor in Molecular Sieve Formation by Dry-Gel Conversion. *J. Am. Chem. Soc.* **2006**, *128*, 6437−6446.
(42) Valenzano, L.; Civalleri, B.; Chavan, S.; Bordiga, S.; Nilsen, M. H.; Jakobsen, S.; Lillerud, K. P.; Lamberti, C. Disclosing the Complex Structure of UiO-66 Metal Organic Framework: A Synergic Combination of Experiment and Theory. *Chem. Mater.* **2011**, *23*, 1700−1718.
(43) Besecker, C. J.; Klemperer, W. G.; Maltbie, D. J.; Wright, D. A. Oxygen-17 Nuclear Magnetic Resonance Spectroscopy of Polyoxometalates. 2. Heteronuclear Decoupling of Quadrupolar Nuclei. *Inorg. Chem.* **1985**, *24*, 1027−1032.
(44) Kubota, Y.; Takata, M.; Kobayashi, T. C.; Kitagawa, S. Observation of Gas Molecules Adsorbed in the Nanochannels of Porous Coordination Polymers by the *in situ* Synchrotron Powder Diffraction Experiment and the MEM/Rietveld Charge Density Analysis. *Coord. Chem. Rev.* **2007**, *251*, 2510−2521.
(45) Ferey, G.; Serre, C. Large Breathing Effects in Three-Dimensional Porous Hybrid Matter: Facts, Analyses, Rules and Consequences. *Chem. Soc. Rev.* **2009**, *38*, 1380−1399.
(46) Walter, T. H.; Oldfield, E. Magic Angle Spinning Oxygen-17 NMR of Aluminum Oxides and Hydroxides. *J. Phys. Chem.* **1989**, *93*, 6744−6751.
(47) Frydman, L.; Harwood, J. S. Isotropic Spectra of Half-Integer Quadrupolar Spins from Bidimensional Magic-Angle Spinning NMR. *J. Am. Chem. Soc.* **1995**, *117*, 5367−5368.
(48) Leung, E.; Mueller, U.; Cox, G.; Hoeffken, H. W. Use of Formate-Based Porous Metal Organic Frameworks for Methane Storage. US 8343261 B2, 2013.
(49) Leung, E.; Mueller, U.; Cox, G. Solvent-Free Production of Magnesium Formate Based Porous Metal-Organic Frame Material. WO 2010106121 A1, 2010.
(50) Samoson, A.; Lippmaa, E.; Pines, A. High-Resolution Solid-State NMR. Averaging of Second-Order Effects by Means of a Double-Rotor. *Mol. Phys.* **1988**, *65*, 1013−1018.
(51) Chmelka, B. F.; Mueller, K. T.; Pines, A.; Stebbins, J.; Wu, Y.; Zwanziger, J. W. Oxygen-17 NMR in Solids by Dynamic-Angle Spinning and Double Rotation. *Nature* **1989**, *339*, 42−43.
(52) Gan, Z. H. Isotropic NMR Spectra of Half-Integer Quadrupolar Nuclei Using Satellite Transitions and Magic-Angle Spinning. *J. Am. Chem. Soc.* **2000**, *122*, 3242−3243.
(53) Blanc, F.; Sperrin, L.; Jefferson, D. A.; Pawsey, S.; Rosay, M.; Grey, C. P. Dynamic Nuclear Polarization Enhanced Natural Abundance ^{17}O Spectroscopy. *J. Am. Chem. Soc.* **2013**, *135*, 2975−2978.
(54) van Eck, E. R. H.; Smith, M. E. Orientation of the Quadrupole and Dipole Tensors of Hydroxyl Groups by ^{17}O Quadrupole Separated Local Field NMR. *J. Chem. Phys.* **1998**, *108*, 5904−5912.
(55) O'Dell, L. A.; Savin, S. L. P.; Chadwick, A. V.; Smith, M. E. A ^{27}Al, ^{29}Si, ^{25}Mg and ^{17}O NMR Investigation of Alumina and Silica Zener Pinned, Sol-Gel Prepared Nanocrystalline ZrO_2 and MgO. *Faraday Discuss.* **2007**, *134*, 83−102.